1-1-2001

Investigation of magnetopause reconnection models using two colocated, low-altitude satellites: A unifying reconnection geometry

A. Boudouridis

Harlan E. Spence
Boston University, harlan.spence@unh.edu

T. G. Onsager

Recommended Citation

Boudouridis, A., H. E. Spence, and T. G. Onsager (2001), Investigation of magnetopause reconnection models using two colocated, low-altitude satellites: A unifying reconnection geometry,J. Geophys. Res., 106(A12), 29451–29466, doi:10.1029/2000JA000350.

JOURNAL OF GEOPHYSICAL RESEARCH, VOL. 106, NO. A12, PAGES 29,451-29,466, DECEMBER 1, 2001

Investigation of magnetopause reconnection models using two colocated, low-altitude satellites: A unifying reconnection geometry

A. Boudouridis

Department of Atmospheric Sciences, University of California, Los Angeles, California, USA

H. E. Spence

Center for Space Physics, Boston University, Boston, Massachusetts, USA

T. G. Onsager

Space Environment Center, NOAA, Boulder, Colorado, USA

Abstract. Ion precipitation data from two co-orbiting Defense Meteorological Satellite Program satellites (F6 and F8) are used to investigate magnetopause reconnection models. We examine differential fluxes between 30 eV and 30 keV, from a Southern Hemisphere, prenoon pass during the morning of January 10, 1990. Data from the first satellite to pass through the region (F6) show two distinct ion energy dispersions ~1° of latitude apart, between 76° and 79° magnetic latitude. The electron data exhibit similar features at around the same region but with no or little energy dispersion, consistent with their high velocities. We suggest that the two energy dispersions can be explained by two separate injections resulting from two bursts of magnetopause reconnection. Data from the second satellite (F8), which moved through the same region 1 min later, reveal the same energy-dispersed structures, only further poleward and with less overall flux. This temporal evolution is consistent with two recently reconnected flux tubes releasing their plasma as they move antisunward away from dayside merging sites. However, an observed overlap between the two ion energy dispersions suggests a more complex reconnection geometry than usual models can accommodate. We propose a generalized reconnection scenario that unifies the Bursty Single X-Line and the Multiple X-Line Reconnection models. A simple time-of-flight particle precipitation model is constructed to reproduce the ion dispersions and their overlap. The modeling results suggest that for time-dependent reconnection the dispersion overlap is observed clearly at low altitudes only for a short period compared with the evolution timescale of the ion precipitation.

1. Introduction

The notion of magnetic reconnection was first applied to the dayside magnetopause by *Dungey* [1961] to explore the process by which mass, energy, and momentum are transferred from the solar wind to the terrestrial magnetosphere. Since then, direct evidence of continuous, quasi-steady reconnection has been obtained [e.g., *Gosling et al.*, 1982]. At the same time, *Haerendel et al.* [1978], reporting on HEOS 2 magnetic field and plasma data, and more extensively *Russell and Elphic* [1978, 1979] using high-resolution ISEE 1 and 2 magnetometer data, suggested that magnetopause reconnection can also occur in a transient, localized manner. *Russell and Elphic* [1978] called this patchy, impulsive reconnection a flux transfer event or FTE. According to their picture, an FTE magnetic signature can be interpreted in terms of a recently reconnected flux tube, created by time-dependent, localized reconnection, sweeping past the spacecraft. An excellent recent review of FTEs can be found in the work of *Elphic* [1995].

The "connected tube" model introduced by *Russell and Elphic* [1978] and later investigated by *Sonnerup* [1987] is not the only model for the description of FTEs. Other models were developed later in an effort to understand the FTE phenomenon and its contribution to flux transfer in the magnetosphere. For a description of all the models currently in existence, see *Scholer* [1995,

Paper number 2000JA000350.
0148-0227/01/2000JA000350$09.00

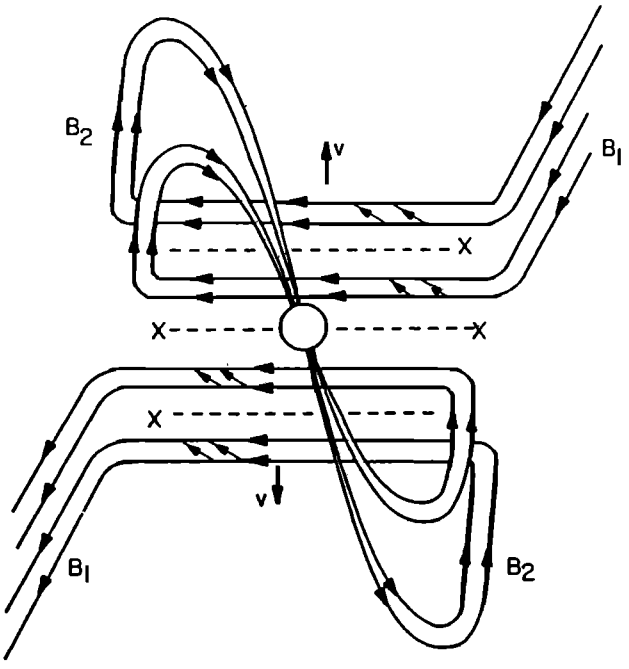

Figure 1. Illustration of the Multiple X-Line Reconnection (MXR) process looking toward the Sun [*Sonnerup,* 1987].

and references therein]. Here we will be concerned with two other models, namely, the Multiple X-Line Reconnection (MXR) model and the Bursty Single X-Line Reconnection (BSXR) model.

The proponents of the MXR model [*Fu and Lee,* 1985; *Lee and Fu,* 1985, 1986; *Shi et al.,* 1988, 1991] envisage the occurrence of magnetic reconnection along several x-lines formed by the tearing mode instability in the magnetopause current layer. Two-dimensional MHD simulations [e.g., *Shi et al.,* 1991] have shown that this type of reconnection results in the creation of magnetic islands at the magnetopause, which grow in time and subsequently convect out of the reconnection region. *Lee and Fu* [1985] suggested that the presence of an interplanetary magnetic field (IMF) B_y component will transform these islands into flux tubes, covering a large longitudinal segment of the dayside magnetopause and resembling the structure of FTEs, as shown in Figure 1 [*Sonnerup,* 1987]. Two important features of FTEs, their intermittence and twisted field structure, are inherent properties of the MXR model. Three-dimensional studies of the flux ropes produced by the MXR model [*Fu et al.,* 1990] indicate that they have "frayed" ends, meaning that the magnetic field at the ends of the tubes connects to both the magnetosheath and magnetosphere in a random way. *Lee et al.* [1993], however, have shown that an appropriate choice of x-line length and distance between x-lines will lead to a preferred connection of the field at the ends of the tube. It should be noted that magnetic flux ropes have also been found to form in the course of three-dimensional semiglobal MHD simulations [*Sato et al.,* 1986; *Ogino et al.,* 1989; J. A. Fedder et al., Flux-transfer events in global numerical simulations of the magnetosphere, submitted to *Journal of Geophysical Research,* 2001].

In the BSXR model, independently developed by *Scholer* [1988a] and *Southwood et al.* [1988], time-dependent reconnection takes place on a single x-line along an extended longitudinal segment of the dayside magnetopause. In their picture, magnetospheric and interplanetary fields connect through a loop-like structure produced by this "bursty" reconnection [*Biernat et al.,* 1987; *Scholer,* 1989] at a specific longitude along the magnetopause. In the presence of either a flow shear across the boundary or an IMF B_y component (or both), the magnetic loop is twisted in the y direction, giving the characteristic twisted field structure observed in FTEs [e.g., *Paschmann et al.,* 1982]. The burst of enhanced reconnection creates a bulge which then moves along the magnetopause because of the tension on the newly opened field lines and the ambient magnetosheath flow, as is illustrated in Figure 2 taken from *Scholer* [1988a]. This bulge distorts the field around it, producing the well-known normal magnetic field FTE signature observed by *Russell and Elphic* [1978] [see *Saunders,* 1983; *Lockwood and Smith,* 1994, hereinafter referred to as LS94].

The main difference of these two models is in terms of the magnetic field connectivity, which in turn is a product of the different reconnection geometries, multiple versus single neutral lines. In the MXR picture

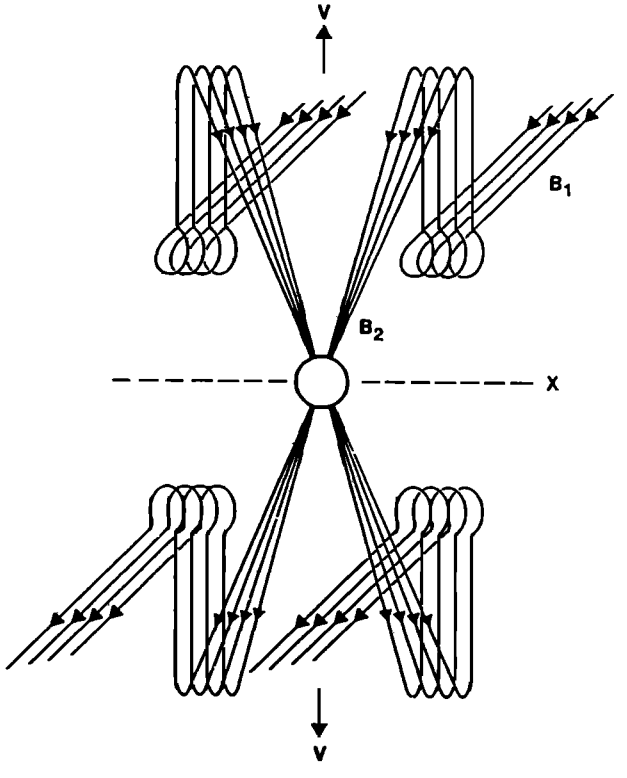

Figure 2. Illustration of the Bursty Single X-Line Reconnection (BSXR) process looking toward the Sun [*Scholer,* 1988a]. Only part of the reconnected lines at the dawnside and duskside are shown for clarity.

the magnetic field of the FTE flux tube connects to either the magnetosheath or the magnetosphere only at the ends of the tube, sometimes doing so erratically as pointed out by *Fu et al.* [1990]. This means that there is a topological connection between different longitudinal segments of the frontside magnetopause. On the other hand, the BSXR model invokes no such topological link, having individual field lines from both sides of the magnetopause connecting over a limited longitudinal extent. Despite their three-dimensional topological differences, the two models share some common features. *Shi et al.* [1991] argued that even though the MXR model depicts reconnection at multiple x-lines, the reconnection rates at these x-lines do not have to be the same. In the case of a much higher reconnection rate at the equatorward line compared with that at the poleward one, a thick layer of singly reconnected field lines will surround the magnetic island formed in the MXR process. This picture is similar to the one predicted by the BSXR geometry. The same authors provide a mechanism for a transistion from multiple to single x-line reconnection by means of locally enhanced resistivity which triggers a higher reconnection rate at the equatorward neutral line.

In this work we present particle precipitation data from two low-altitude, co-located Defense Meteorological Satellite Program (DMSP) satellites as they passed through low-altitude reconnection signatures. We argue that a full interpretation of the data requires a combination of both the MXR and the BSXR models. We show that the two factors mentioned above, the field topology and the extent of the neutral lines, play an important role in understanding the low-altitude particle signatures of dayside magnetopause reconnection. Section 2 gives an overview of the data and any additional information used. Section 3 describes the reconnection picture, while section 4 presents the results of a simple time-of-flight precipitation model used to reproduce the data ion dispersions. Finally, section 5 discusses the conclusions of our work.

2. Data Description

The two DMSP satellites used in this study, F6 and F8, are in Sun-synchronous, circular polar orbits and are virtually co-orbital in the dawn-dusk plane; their cross-track separations rarely exceed 50 km at auroral latitudes. They both fly at altitudes between 800 and 900 km. A slight difference in their semimajor axes yields a fractional difference in their orbital periods; they differ by less than 40 s out of ~101 minute periods. This leads to a racetrack effect in which the faster satellite (F6) "laps" the slower satellite (F8) regularly. The resonant interaction time is ~11 days. Near closest approach their in-track separation gradually reduces to a minimum of ~10 km, thereby offering for the first time simultaneous sampling of the low-altitude space particle environment at two nearly co-located positions. The utility of these data sets has already been demonstrated for case studies of auroral particle precipitation [*Watermann et al.*, 1993; *Jorgensen and Spence*, 1997; *Jorgensen et al.*, 1999].

The auroral crossing we study here occurred during a Southern Hemisphere polar pass, around 1040 UT, on January 10, 1990. The spacecraft moved from high to low latitude, in the dawnside of the polar ionosphere, and F6 was leading F8 with a time lag of ~60 s. The orbit tracks of the satellites in magnetic coordinates are shown in Plate 1. They are so close that their individual tracks merge. The color band to the left of the orbits indicates the time lag between the two spacecraft at every point along the orbit, translated in seconds using the color scale at the bottom right. The colors on the orbits themselves refer to the signatures of the different magnetospheric regions encountered (cusp, low-latitude boundary layer (LLBL), plasma sheet, and "other"), which are described to the right of the plot. These regions were determined from the observed particle fluxes, using a modified version of the original Newell-Meng criteria for region identification [*Newell and Meng*, 1988], in which priority is given to the cusp/LLBL identification instead of the plasma sheet one.

The precipitating particle fluxes were obtained by the Geophysics Laboratory SSJ/4 instruments flown on both the DMSP F6 and F8 spacecraft. These sensors have their look directions always oriented radially away from the Earth. They are identical in design, measuring the flux of precipitating electrons and ions in 20 energy channels, logarithmically spaced over the energy range of 30 eV to 30 keV. Their duty cycle yields a complete 20-point electron and ion spectrum once per second. It corresponds to a spatial resolution of ~7 km along the orbital track. For a more detailed account of the instruments and their specifications, see *Hardy et al.* [1984].

In this paper we focus primarily on ion fluxes, but we also present the electron data for completeness. Plate 2 shows magnetic latitude series of integral and differential energy fluxes, from both F6 and F8, for ions (a) and electrons (b), on a magnetic latitude grid with resolution of 0.05°. The line color of the integral fluxes has the same meaning as in Plate 1.

Two energy-dispersed features can be seen in the ion data from the F6 spacecraft (top two pannels of Plate 2a) with equatorward edges at 76.4° and 77.2° magnetic latitude. Each extends poleward by several degrees. These regions satisfy the Newell-Meng cusp identification criteria. These well-known ion dispersions are the result of the velocity filter effect in which lower energy particles injected at the same location with higher energy ones will arrive at low altitudes at progressively higher latitudes due to the poleward convection of the field lines during southward IMF conditions [*Rosenbauer et al.*, 1975]. Similar features appear also on the F8 ion data (bottom two pannels of Plate 2a),

which passed through the same region a minute later. From F8 we can immediately see that the equatorward edges of the ion dispersions have moved poleward to 76.7° and 77.5° magnetic latitude, respectively. This reveals a poleward motion of the energy dispersions of ~0.3° per minute or a corresponding latitudinal velocity of 600 m s^{-1}.

The conditions prevailing in the solar wind during our observations are of great importance for an accurate interpretation of the data, as will be highlighted in section 3. Measurements from the IMP 8 spacecraft, located at around $X_{GSM}=-15\ R_E$, give the magnitude of the three IMF components as $(B_x, B_y, B_z)=(-5\,nT, +8\,nT, -3\,nT)$, which were steady throughout the event. The solar wind dynamic pressure was around 3 nPa. Our low-altitude observations are therefore during southward IMF conditions with a big B_y component, both favorable for magnetic reconnection of the types discussed in section 1 and again in the context of this event in the next section.

3. Reconnection Scenario

Our reconnection scenario implements the basic principles of two earlier ideas: the BSXR model of *Scholer* [1988a] and *Southwood et al.* [1988] and the MXR model of *Lee and Fu* [1985]. The BSXR model is used to give an initial interpretation of the ion data, while the MXR model is invoked to explain the topological discrepancies arising from a closer inspection of the observed ion dispersions.

3.1. BSXR Only

Smith and Lockwood [1990] suggested that the low-altitude particle signature of time-dependent reconnection at the magnetopause is a "pulsating cusp." Adopting the principles of the BSXR mechanism, they argued that a burst of enhanced reconnection will result in the formation of a plasma "bubble" extending in longitude along the magnetopause, which will then release its particles, observed in the form of dispersed signatures at low altitudes. *Cowley et al.* [1991b] and *Smith et al.* [1992] predicted that the result of the intermittence of reconnection at the magnetopause will be discontinuous changes in the ion precipitation characteristics at low altitudes. More specifically, they suggested that sudden jumps will appear in the low-energy cutoff of the ion dispersive features due to changes of the reconnection rate at the subsolar point. *Newell and Meng* [1991] observed these sudden energy transitions in ion cusp spectrograms from the DMSP F7 satellite (giving them a spatial rather than temporal interpretation), and *Lockwood and Smith* [1992] devised a method to deduce the reconnection rate variations from the ion energy-time spectrogram. Applying their method to one of the *Newell and Meng* [1991] spectra, they concluded that reconnection occurs in a series of short bursts bounded by periods of little or no reconnection.

Following the above picture, each one of the two energy dispersions seen in Plate 2a can be attributed to a distinct reconnection event. The two open flux tubes, formed in this way, release their magnetosheath plasma to the ionosphere as they evolve and convect antisunward. The addition of an IMF B_y component to this picture will slightly modify the details of the motion, but its main characteristics remain unchanged. As pointed out by *Smith and Lockwood* [1990], a nonzero B_y will impart an east-west component to the initial motion of the feet of the reconnected field lines around the polar cap boundary due to the asymmetric tension on the lines. Thereafter the lines are swept tailward by the magnetosheath flow around the magnetopause. Taking these effects into account in our case, we would expect the positive IMF B_y to move the ion dispersions toward the noon meridian in Plate 1 (which includes the poleward motion of the features, seen in Plate 2a). This picture is consistent with high-latitude dayside ionospheric convective flows under the presence of an IMF B_y component [*Cowley et al.*, 1991a] (see also the cusp review by *Smith and Lockwood* [1996]).

3.2. Overlapping Dispersions

At first glance the ion data seem to be in agreement with the BSXR process and the pulsating cusp model. A closer look at the data, however, reveals one significant detail that this model alone cannot reproduce. The two ion energy dispersions overlap with each other, on both F6 and F8 data. The overlap occurs between 77.2° (77.45°) and 77.7° (77.6°) in the F6 (F8) data (see Plate 2a). This naturally raises the question, how can two different plasma injections populate the same field lines? The BSXR model predicts them to be completely separated, bounded by explicitly distinct field lines (see Figure 2 of *Lockwood and Davis* [1996], hereinafter referred to as LD96). Therefore they either have crossed into each other's "domain" after reconnection (violating the frozen-in condition) or have formed on common field lines at separate but topologically connected reconnection sites.

Overlapping injections of magnetosheath ions have attracted much attention in recent years. First observed by *Carlson and Torbert* [1980] in rocket experiments, they have also recently been detected at midaltitudes by the Viking satellite [*Woch and Lundin*, 1991, 1992; *Yamauchi and Lundin*, 1994]. LS94 interpreted these overlaps as a finite gyroradius effect and stressed that no overlap should be observed for the field-aligned precipitating particles, in good agreement with the absence of these features in low-altitude ion data from the DE 2 or DMSP satellites. The same year, however, overlapping features were reported by *Norberg et al.* [1994] in low-altitude data taken by the Freja satellite.

In an effort to explain these observations, *Lockwood* [1995a] came up with a new mechanism that can cause overlaps even for the zero pitch angle particles, based

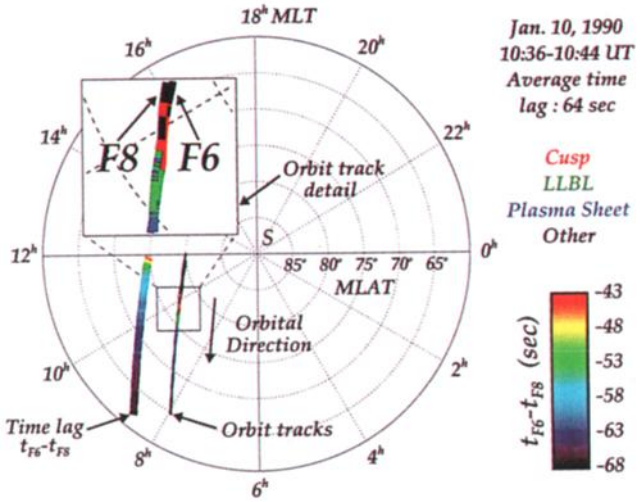

Plate 1. DMSP satellite orbits over the southern polar cap. The two tracks are almost identical. The color band to their left indicates the time lag between them, given in seconds by the color scale to the bottom right. The magnetospheric regions are also identified with the colors on the tracks themselves.

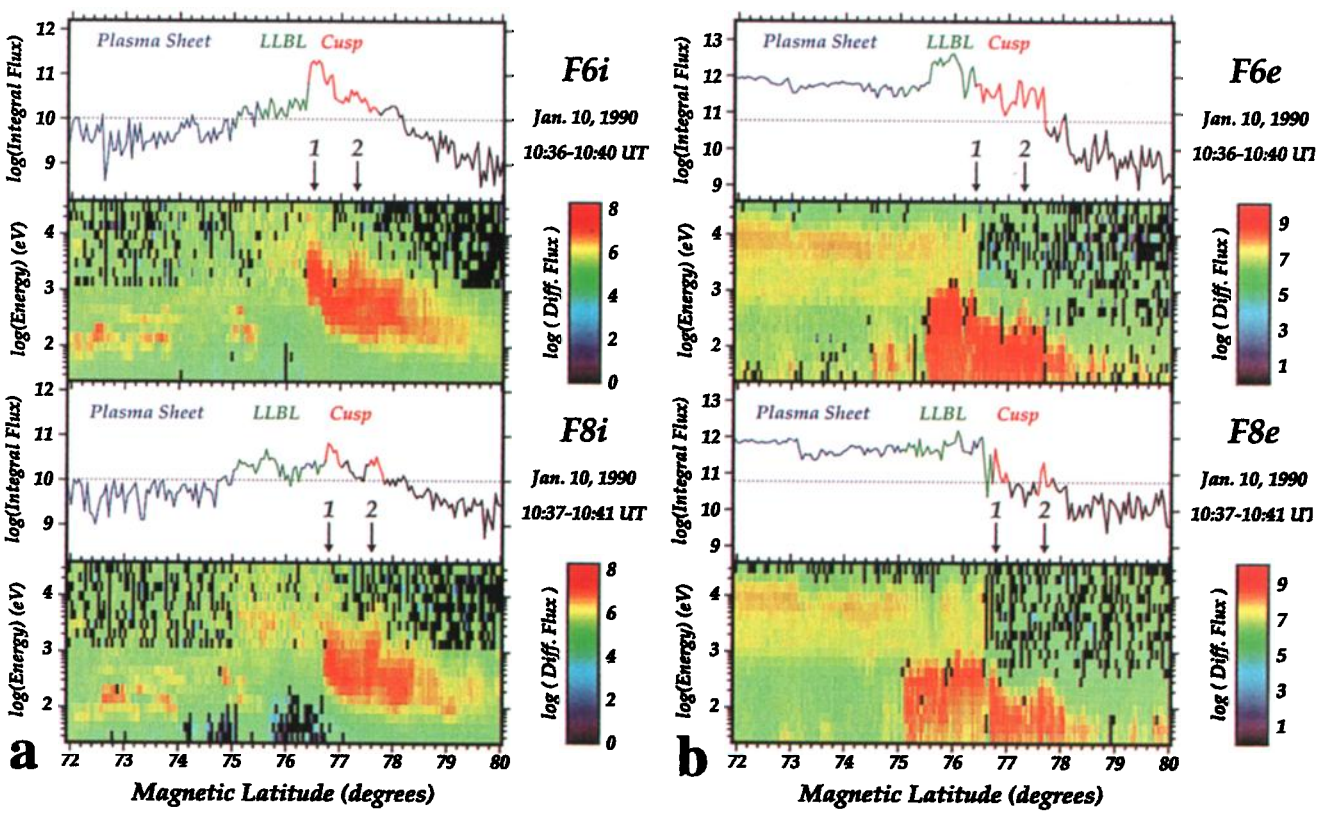

Plate 2. Integral and differential ion (a) and electron (b) energy fluxes. The line color of the integral fluxes corresponds to the regions shown immediately above. The arrows point the location of the high-energy part of the energy dispersions.

on the combined effects of ion acceleration immediately after reconnection, straightening of field lines, and ion time of flight. According to his mechanism, a preexisting single dispersion at some point bifurcates, with low- and high-energy particles present but little or no intermediate energy ones. Later on, the two energy-separated parts merge again in a single dispersion. Any change in the reconnection rate restores the bifurcated conditions, causing sudden jumps for both or at least the high-energy portions of the ion dispersion. However, this does not seem to be the case in our event. *Lockwood* [1995b, p. 21,799] pointed out that the bifurcated structure "only arises for field lines which accelerate over a sufficient distance of the magnetopause before straightening." This requires reconnection to occur at fairly low, subsolar latitudes (or even the opposite hemisphere for extreme cases). As discussed in section 4, our reconnection event likely occurred near the southern cusp, allowing little or no acceleration (before straightening) for the newly reconnected field lines.

Using data from the Polar satellite, *Fuselier et al.* [1997] observed bifurcated ion signatures in which the high-energy component exhibits the usual energy-latitude dispersion but the low-energy one is dispersionless. Following the suggestion of *Yamauchi and Lundin* [1994], they attributed the overlap to re-reconnection of a single magnetospheric line at different points with different components of a highly draped IMF. Each one of the two observed overlapping energy components is then due to a separate particle injection at two different reconnection events on the same field line, although it is not clear why the low-energy one appears dispersionless. Finally, *Trattner et al.* [1998], reporting also on Polar observations, identified a different kind of overlapping signature, one that does not evolve from a preexisting single dispersion but rather exhibits random appearance and disappearance of overlapping energy bands, sometimes above and below an original steady trace. Because of the absence of jumps in the energy of these traces and the occasional presence of a stable original trace, they concluded that steady reconnection conditions must prevail at the magnetopause. They added that the transient nature of the energy overlap might suggest multiple injections on the same field line (i.e., re-reconnection), lending support to the model discussed by *Fuselier et al.* [1997], although the data are still inconclusive as to the exact mechanism.

In the above reported models of field-aligned, overlapping ion energy features, the overlap begins at the same point in space for both energy components, indicating either a single injection with missing intermediate energies [*Lockwood,* 1995a] or successive injections on the same geomagnetic field line [*Fuselier et al.,* 1997]. Our ion dispersions differ from the above in that they have well-separated onsets in latitude, both at similar energies, but the poleward low-energy edge of the equatorward dispersion overlaps with the high-energy onset of the poleward one, excluding a pure BSXR generating mechanism at the same time. This suggests two distinct injection events on originally different magnetospheric field lines which subsequently become topologically connected to each other, mapping down to the same region on the high-latitude ionosphere.

Additional evidence for the two-injection theory comes from the electron spectra of Plate 2b. They also show two separate injections at almost the same positions as the ions, with the same separation and similar poleward motion. The electron data also reject the possibility of contamination of the ion detector by heavier ions, which if present could be responsible for the second ion dispersion, as suggested by *Burch et al.* [1982]. In the case of a single injection which splits into two in the ion spectra due to different ion species, one injection should have been observed in the electron spectra, which is not true here.

Xue et al. [1997] attempted to account for two seemingly separate overlapping injections, seen in the midaltitude Viking data [e.g., *Yamauchi and Lundin,* 1994] for all pitch angles, by means of magnetosheath plasma density fluctuations coupled with a steady state reconnection. By allowing the magnetosheath plasma density to fall for a specific time interval and then return to its original high value, and assuming that different energy zero pitch angle particles on the same field line come from different points along the magnetopause [e.g., *Onsager et al.,* 1993], they produced a simulated overlapping signature in which a band of low particle flux appears at middle energies due to the mapping of these particles to the low-density magnetosheath during the density reduction. They pointed out, however, that a clearly observed overlap would require a strictly limited range of duration for the magnetosheath density variation (~1 min). Too short an interval (of the order of seconds) would result in the merging of the two energy components, while too long an interval (~2 min) would lead to energy dispersions well separated in latitude and hence not overlapping, especially for the field-aligned particles.

Even though this mechanism has the potential of producing overlapping features at low altitudes, it does not seem to be the source of our DMSP overlapping ion dispersions. The fortuitous two-point nature of our data can reasonably exclude this hypothesis. Since the time lag between the two measurements is 1 min, if the duration of the proposed density decrease had been less than 1 min, one spacecraft would have fallen outside the flux reduction effect and thus would have observed a single continuous dispersion. On the other hand, if the duration had been more than 1 min, the overlap observed would have been almost nonexistent. The obvious invariability of the two ion dispersions in both latitudinal extent and energy structure requires a different interpretation of the apparent overlap.

All the studies previously conducted on the subject of overlapping dispersions, including the currently proposed one, are summarized in Table 1. Before we offer

Table 1. Overlapping Dispersion Studies

Authors	Spacecraft	Altitude	IMF	Mechanism
Woch and Lundin [1992]	Viking	midaltitude	mainly radial (small B_y)	finite gyroradius LS94
Norberg et al. [1994]	Freja	low altitude	assumed southward	bifurcation *Lockwood* [1995a]
Yamauchi and Lundin [1994]	Viking	midaltitude (all angles)	roughly southward	magnetosheath density variations *Xue et al.* [1997]
Fuselier et al. [1997]	Polar	midaltitude (all angles)	$(-B_x, +B_y, -B_z)$	re-reconnection
Trattner et al. [1998] First event	Polar	midaltitude (all angles)	$(+B_x, +B_y, \approx 0)$	re-reconnection or bifurcation?
Trattner et al. [1998] Second event	Polar	midaltitude (all angles)	$(-B_x, +B_y, -B_z)$	re-reconnection or bifurcation?
Current study	DMSP F6/F8	low altitude	$(-B_x, +B_y, -B_z)$	BSXR and MXR[a]

[a]BSXR, Bursty Single X-Line Reconnection; MXR, Multiple X-Line Reconnection.

a new mechanism for the generation of ion overlapping dispersions, we want once again to underline the significance of the IMF orientation in any intercomparison between the processes producing them. Different IMF orientations will result in substantially different reconnection geometries [*Luhmann et al.*, 1984; *Crooker et al.*, 1985; *Crooker*, 1986], giving a range of possible overlap-causing mechanisms taking place during entirely different conditions, one not necessarily invalidating another.

3.3. BSXR and MXR

We propose a new overlap-producing mechanism based on the concept of pulsed reconnection at the magnetopause, but one that does not strictly adhere to the BSXR model. Instead, both the BSXR and the MXR models are involved in this mechanism, with different temporal and spatial scales, together with different contributing reconnection rates. The idea of two coexisting reconnection processes is old. Many authors [*Cowley*, 1982; *Rijnbeek et al.*, 1984; *Lockwood and Smith*, 1992; 1994; *Pinnock et al.*, 1995] have discussed the possibility of continuous and time-dependent FTE-like reconnection occurring simultaneously at the magnetopause. They noted that bursts of enhanced reconnection can take place on top of a low-level, background continuous reconnection. *Cowley* [1982] suggested that steady state and impulsive reconnection processes may both be part of a continuous spectrum of reconnection space and time scales.

We take the idea of coexisting reconnection processes a step further by suggesting that the MXR process forms the low-level, background component while bursts of enhanced flux transfer of the BSXR type are superimposed on it. Following *Lee and Fu* [1985], a spatially constant, low resistivity gives rise to low-level reconnection at multiple x-lines. The magnetic islands form and slowly move poleward and in the dawn-dusk direction, owing to the tension on the open field lines and the presence of an IMF B_y component. In this way there is a continuous topological link for the entire frontside magnetopause.

The process is illustrated in Figure 3 in a sequence of schematic snapshots of the background reconnection regime, as seen from the Sun. Two multiply reconnected field lines (thicker solid lines) are formed, one in each row of panels. The first panel of each row depicts the prereconnection picture, the second depicts the reconnection occurring first at the primary x-line at the center, and the third depicts the follow-up reconnection at the secondary x-lines above and below. The first, evolved, multiply reconnected line is retained in the second row, to demonstrate the formation of the MXR background. The thin solid lines denote all the other field lines involved in the process, while the thin dotted lines are the original dipole line positions. Following reconnection, the magnetic tension pulls the lines poleward and in the dawn-dusk direction. This is a simple illustration of the field topology which ignores some of the details of MXR like the tilted x-lines due to the IMF B_y component [*Lee and Fu*, 1985; *Crooker*, 1986].

In addition to this low-level process, the presence of a localized and time-dependent enhanced resistivity at

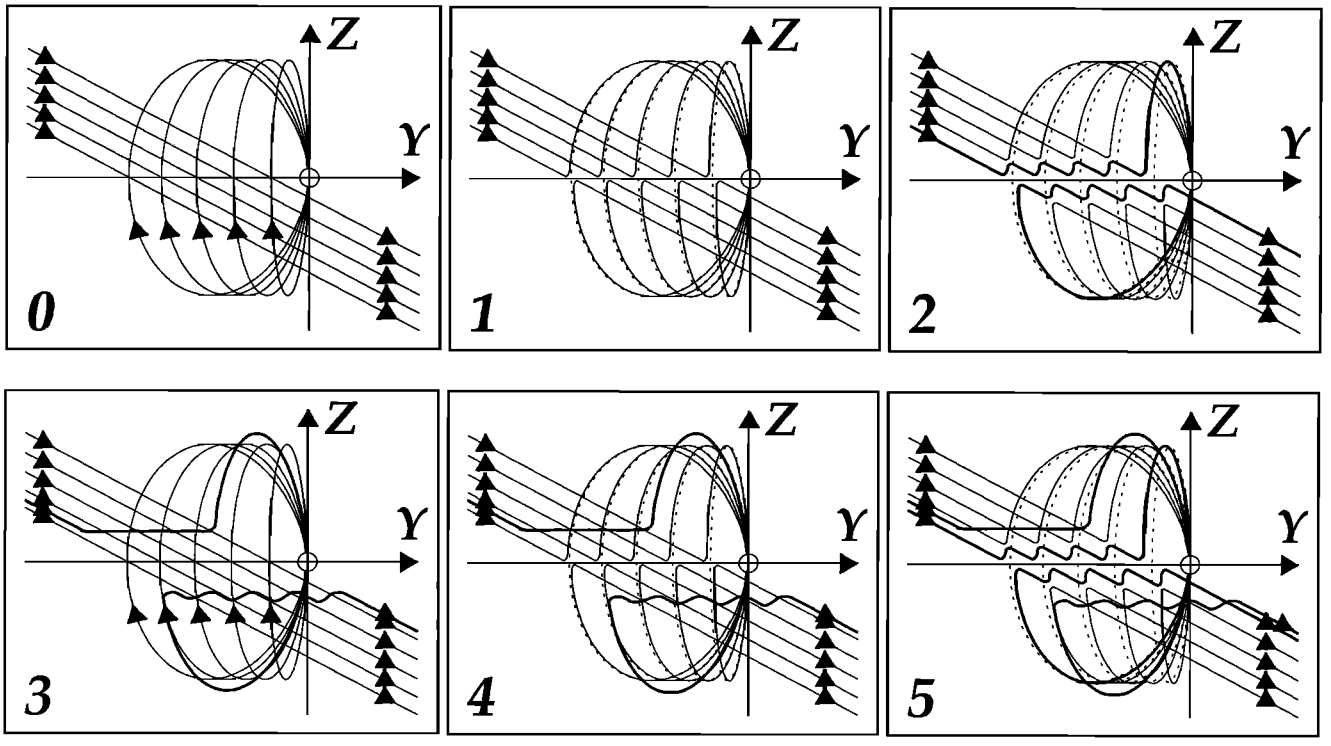

Figure 3. Six snapshots illustrating the formation of two multiply reconnected field lines (thicker solid lines) seen from the Sun, one row of panels for each line.

the central, primary neutral line will modulate the rate of reconnection there, switching to the BSXR mechanism in the way outlined by *Shi et al.* [1991]. A layer of singly reconnected field lines will form, piling up around the multiply reconnected ones and sweeping them along as they move more or less in the same direction. This may partly account for the strong core magnetic field observed in FTEs in a way similar to that proposed by *Scholer* [1988b]. The field configuration in this case will be the result of a superposition in space of the fields shown in Figures 1 and 2, with the singly reconnected field lines engulfing the multiply reconnected ones. Since most hot ions in the BSXR model reside in the center of the plasma structure formed by it [e.g., *Southwood et al.*, 1988], they will find themselves on multiply reconnected lines and therefore escape along these lines down toward the ionosphere. *Fu et al.* [1990] observed these enhanced tube-aligned flows in their three-dimensional MXR simulations.

But how can this unifying model account for the ion dispersion overlap? If the burst of reconnection at the primary x-line is confined to a small longitudinal segment, then a number of plasma "blobs" of this type can form at the same time but at different longitudes. Thereby, all of them map down to a common ionospheric footprint of the interconnecting multiply reconnected field lines produced by the background MXR process. While the issue of the longitudinal extent of individual reconnection events is still highly contested (see LD96 and references therein), our model adopts the patchy BSXR picture. For the record, patchy merging has also been invoked in the context of other reconnection mechanisms, like MXR [*La Belle-Hamer et al.*, 1988] or component merging at multiple off-equatorial sites [e.g., *Kan*, 1988; *Nishida*, 1989].

Furthermore, if the onsets and durations of the BSXR events that produce these plasma blobs do not exactly match, the blobs will be only partially threaded by the same field lines, allowing any degree of overlap between the resulting ion energy dispersions at low altitudes. The first plasma injection will have the poleward low-energy edge of its dispersion appearing further poleward of the ones forming at later times. This picture is schematically illustrated in Figure 4, in a format similar to that of Figure 3. Figure 4a shows the view from the Sun of magnetopause field lines, while Figure 4b shows their projection to the ionosphere. Two finite-size plasma blobs, 1 and 2, bounded between the MXR-produced lines (B,D) and (A,C) respectively, will overlap between the points B′ and C′ in the ionosphere. "A" is the oldest line, and "D" is the newest one.

4. Dispersion Model

In this section we demonstrate the ability of the above unifying reconnection model to produce the observed overlap of the ion energy dispersions and its temporal evolution, using a simple time-of-flight precipitation model. The key element in our calculation is the fact that unlike the previous time-dependent reconnection

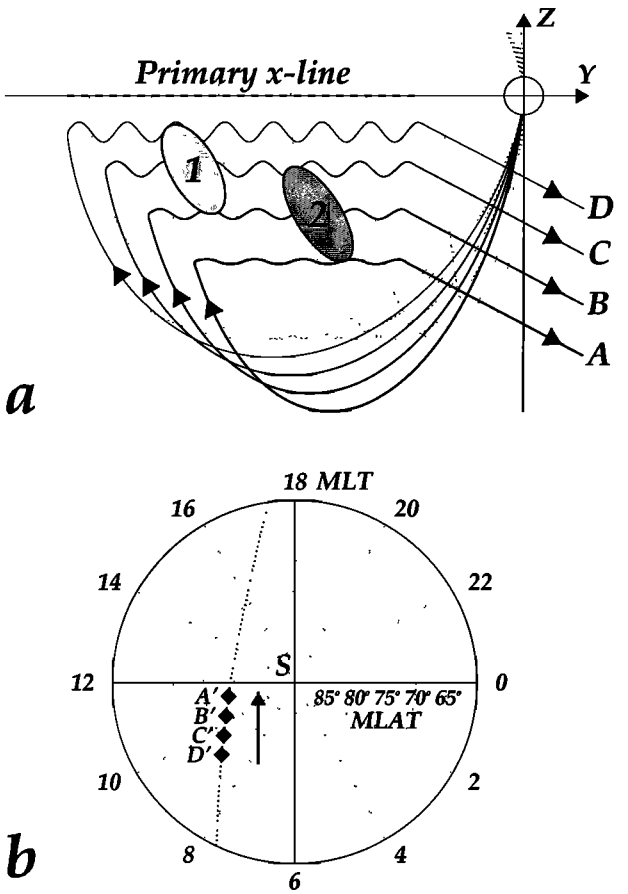

Figure 4. Reconnection snapshot illustrating the mechanism producing the overlap of the ion energy dispersions. (a) The plasma "blob" locations at the magnetopause, viewed from the Sun with Earth at the upper right corner. (b) The respective feet in the polar ionosphere of the field lines bounding them. The arrow indicates the apparent motion of the energy features. The overlap occurs between the lines B and C, connecting to B′ and C′, respectively, in the ionosphere.

models (e.g., LS94, LD96) which use a single, variable reconnection rate, our reconnection scenario allows the independent modeling of the reconnection rate at each spatially separated location, marked by the blobs 1 and 2 in Figure 4. In doing so, the observed overlap of the resulting ion dispersions can be reproduced easily.

4.1. Dispersion Modeling Background

Single, nonoverlapping ion dispersions have long been observed in the high-latitude plasma mantle [*Rosenbauer et al.*, 1975] and the magnetospheric cusps [*Reiff et al.*, 1977]. The magnetosheath-like plasma content was one clue to their association with magnetopause reconnection. Their spectral characteristics result from bulk tailward motion (under southward IMF conditions) of newly open field lines, owing to the combined effect of magnetic tension and tailward magnetosheath flow. This velocity filter effect leads to the formation of the well-known low-energy ion cutoff of the ion energy dispersions. It constitutes a powerful tool for investigating the properties of the magnetopause reconnection site [*Lockwood and Smith*, 1992; *Phillips et al.*, 1993; *Newell and Meng*, 1995; *Lockwood*, 1995b]. Along with decreasing ion energy with increasing latitude, a drop of the ion flux is also observed [e.g., *Newell et al.*, 1991]. This is a result of the variation of magnetosheath properties along the magnetopause [*Spreiter and Stahara*, 1985] and the realization that as a consequence of the tailward convection of the open field lines, magnetosheath plasma crosses the magnetopause continuously at a large range of locations [*Onsager et al.*, 1993; LS94].

Several models of the above process and resulting energy dispersions exist. *Onsager et al.* [1993] combined three different modules to associate low-altitude particles with the magnetosheath phase space density. Assuming Maxwellian distributions in the magnetosheath, they calculated the particle fluxes at the magnetopause and, through Liouville's theorem and model fields, the fluxes in the low-altitude precipitation regime. Subsequently, *Onsager et al.* [1995] revised this model using improved magnetic and electric fields and compared the results with both high- and low-altitude observed spectra. The measured ion flux and energy behavior were modeled sufficiently well at both altitudes. One notable discrepancy was that the cusp location systematically appeared at latitudes significantly higher than those observed in the data. *Newell and Wing* [1998] introduced further improvements, including the use of Kappa distributions instead of Maxwellians, an upgraded magnetic field model, and more realistic ionospheric convection velocities, resulting in a proper geolocation of the cusp.

The models discussed so far, called "Onsager-class" models by *Newell and Wing* [1998], treat the entire high-latitude dayside precipitation environment, from the open LLBL to the cusp and the plasma mantle, as a consequence of quasi steady state reconnection at the magnetopause. This produces ion energy dispersions which progress smoothly from LLBL to cusp to mantle morphology, like the examples presented by *Newell and Meng* [1995]. Any discontinuities appearing in the ion dispersions were attributed to spatial rather than temporal effects [*Newell and Meng*, 1991; *Onsager et al.*, 1995].

The explicit inclusion of temporal variations of the magnetopause reconnection rate in models was first introduced by LS94 for the high- and low-energy cutoffs of the low-altitude ion spectra, then subsequently by LD96 for the complete ion spectrum. As mentioned in section 3.1, this idea was based on the pulsating cusp model of *Smith and Lockwood* [1990] and the prediction and observation of discontinuous jumps in the ion energy dispersion characteristics, the so-called "staircase" signature [*Escoubet et al.*, 1992]. These signatures

were reproduced in the above models for both discrete reconnection pulses with zero reconnection in between (LD96) and bursts of enhanced reconnection on top of a low-level background (LS94). Similar results were also obtained for midaltitude cusp data [*Lockwood et al.*, 1998] and various orientations of a low-altitude spacecraft orbit with respect to the open-closed boundary (OCB) (LD96).

4.2. Time-of-Flight Precipitation Model

We present here the results of a simple precipitation model that reproduces the observed ion energy dispersions. We discuss the model only qualitatively, with a more quantitative description to be presented elsewhere. In contrast to previous precipitation models, no particle tracing in prescribed magnetic and electric fields [*Onsager et al.*, 1995; *Newell and Wing*, 1998] or rigorous treatment of magnetosheath properties (*Lockwood*, 1995b; LS94) are applied. Rather, simplified magnetosheath conditions are used to best reproduce the spacecraft measurements, from which essential elements of the process can be understood. It is based on time-of-flight arguments, the time and energy dependence of the magnetosheath particle flux, and the effects of temporal variations of magnetopause reconnection.

In their review of low-altitude cusp particle signatures, LS94 concluded that once a field line is opened, there will be a continuous entry of magnetosheath particles into the magnetosphere, all along the magnetopause as this line convects antisunward by the solar wind flow. In this work we use a simpler but conceptually similar approach, proposed initially by *Smith and Lockwood* [1990] in the context of the BSXR model. In their view a cylindrically shaped flux tube of finite width reconnects along some longitudinal extent at the magnetopause during some finite time interval, after which reconnection ceases. The plasma "blob" created by this burst of reconnection then moves antisunward while retaining its shape and initially without releasing its particles, as shown in Figure 5 [from *Smith and Lockwood*, 1990]. At some later point the particles are released, precipitate, and are observed as energy-dispersed features at low altitudes.

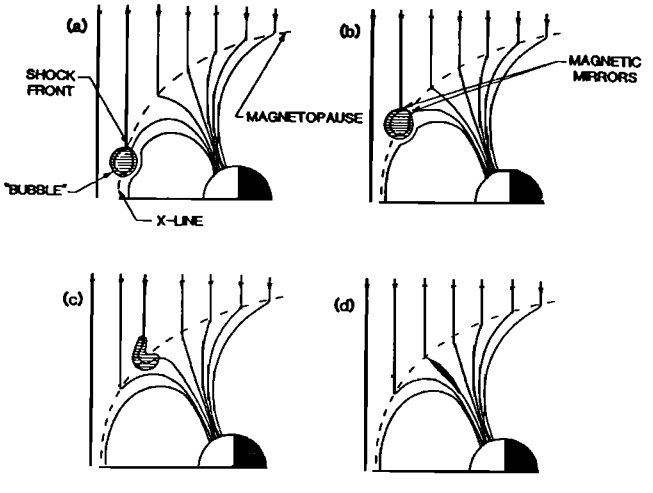

Figure 5. Plasma blob motion after reconnection, in a meridional cut looking from dusk (called "bubble" by *Smith and Lockwood* [1990]).

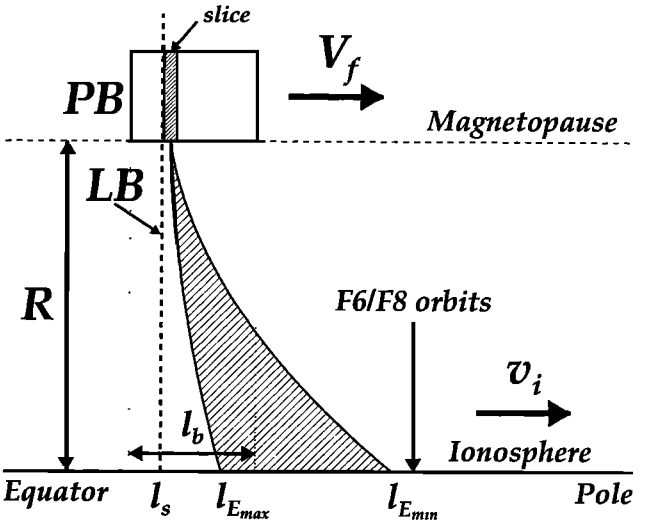

Figure 6. A schematic drawing illustrating the loss process. PB, plasma blob; LB, loss boundary. R is the distance from the spacecraft to the PB kept constant at all times, V_f and v_i are the velocities of the blob at the magnetopause and the ion dispersions in the ionosphere, respectively. See text for more details.

We should point out that their assumption of a confined, finite plasma blob is highly idealized. Nevertheless, even though the magnetosheath provides a constant source of particles, the hot, dense particles that only exist near the subsolar region can be modeled as a finite volume source. Furthermore, the simplicity of the model based on this picture facilitates demonstration of the BMXR mechanism, so we adopt this framework.

Each ion dispersion in Plate 2a is modeled as the result of the time evolution of a finite width plasma blob of the type proposed by *Smith and Lockwood* [1990]. The conceptual model is illustrated schematically in Figure 6. The frozen-in condition is observed; that is, the field lines move at the same speed as the plasma blob (PB). Owing to tension produced by the IMF B_y component, flux tubes and the energy dispersions will move toward noon. In the model, however, we are concerned only with the latitudinal component of the inferred motion.

Precipitation starts when the leading edge of the flux tube reaches a conceptual boundary we call the "loss boundary" (LB), equivalent in reality to the OCB in terms of particle precipitation. It is the point where plasma containment is lost and particles are released, and it maps to the satellite altitude at a latitude l_s. We separate each blob into perpendicular-to-its-motion slices that lose particles independently from neighboring

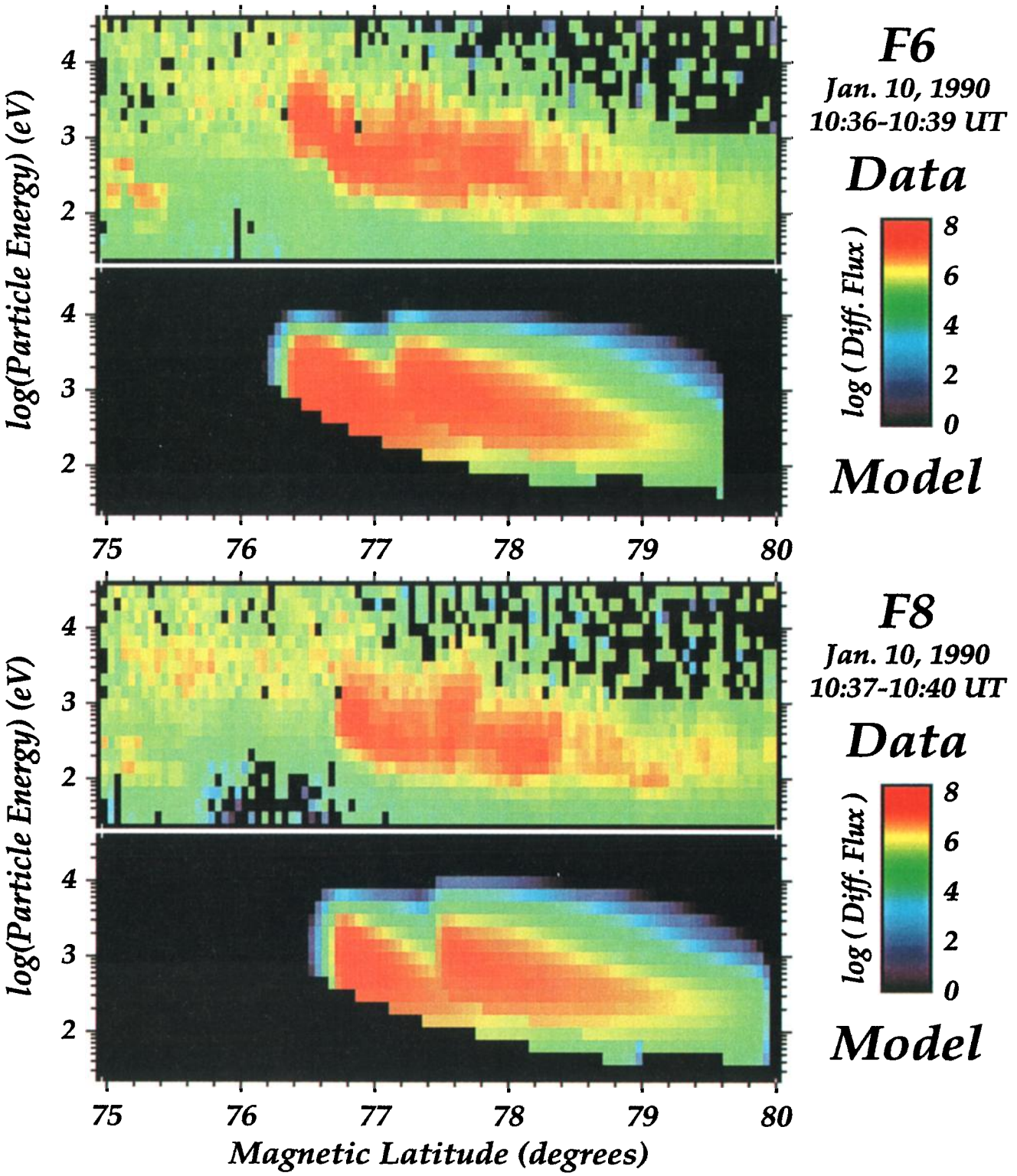

Plate 3. Model results for both dispersions.

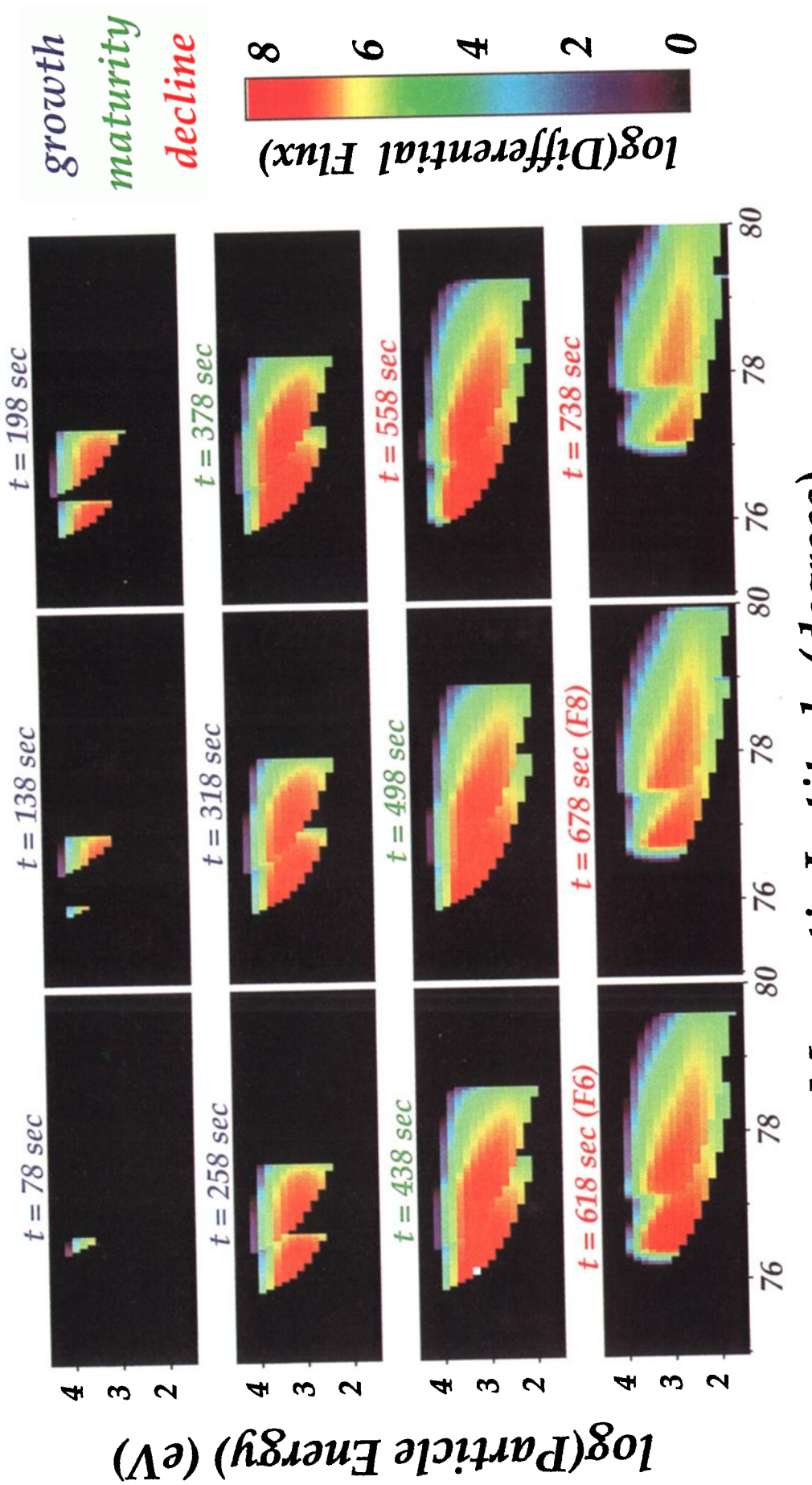

Plate 4. Temporal evolution of the ion dispersion model for both dispersions on the same time frame. Each frame belongs to one of the three dispersion phases shown to the right and are color-coded with the time since reconnection above the frames.

slices. This reflects the frozen-in assumption. Every slice that reaches the LB starts losing particles with a rate $r(t, E)$, which in essence describes the particle flux at this point in the magnetosheath. The particle distribution function in each slice is assumed to be a truncated convecting Maxwellian [*Cowley,* 1982] with temperature T_b and density n_b common for the entire blob. The energy flux reaching the satellite is directly related to the loss rate at the blob (through Liouville's theorem), taking into account the travel time of the particles.

Note that the hatched area of Figure 6, denoting the precipitating particles, serves only to highlight the locus of particle arrival in the ionosphere according to their energy at later times, not the time when the respective slice crosses the LB. At any time, precipitation occurs only between the two field lines (dotted lines) bounding the blob, if the time-of-flight requirement applies. This requirement is imposed by the assumption of temporal variations of the reconnection rate at the magnetopause, which create a finite-size PB mapping to a latitudinal extent l_b at the ionosphere.

4.3. Model Results

The above model is used to simulate the two ion dispersions seen in the F6 data of Plate 2a. Parameters were fixed through fits to the observations. Using the F6-derived parameters, we let the model evolve temporally until the time of the F8 data, where the model–F8 data match is examined. We assume that all dispersions move with the same constant latitudinal velocity $v_i = 600$ m s^{-1} deduced earlier through comparison of F6 and F8 data. The results are shown in Plate 3. The model simulates the two ion dispersions remarkably well. The flux and low-energy ion cutoff evolution with magnetic latitude and hence time since reconnection are rendered with sufficient accuracy. The steep low-latitude edge corresponds to the temporal variation of reconnection, while the extended low-flux, high-latitude edge results from the tailward acceleration of the field lines.

The observed overlap between the two dispersions, which was the main point pursued here, is also easily recognized in the model results for both spacecraft. The apparent reduction of this overlap with time, between the F6 and F8 data, arises naturally in the model due again to the transient nature of reconnection. Following cessation of reconnection at the magnetopause, the equatorward edge of the ion dispersion moves along with the last reconnected field lines at the same ionospheric velocity. Its poleward edge moves with the same speed, but its energy flux at significant levels (red color in Plate 3) remains more or less stationary. So even though the actual overlap remains constant, the ability to observe the overlap decreases with time. While the high-flux equatorward edge of the second dispersion moves, the high-flux tail of the first one remains virtually unchanged.

Another interesting result of the model is the low values of R (8–9 R_E) for both dispersions. These were determined by a visual match of the low-energy ion cutoff from the data and the model. They were later confirmed by a more rigorous treatment to be presented in a future publication. They indicate an initiation of particle precipitation, or alternatively reconnection itself, at high latitudes near the southern cusp, rather than at low (i.e., subsolar) latitudes. This conclusion is supported by the high values of the boundary-tangential magnetosheath flow speed in the plane of the sheath field near the x-line. The resulting sheath velocities of -210 and -110 km s^{-1} for dispersions 1 and 2, respectively, are suggestive of a high-latitude reconnection site as opposed to a low-flow, low-latitude one [*Lockwood et al.,* 1995].

4.4. Temporal Evolution

As mentioned in section 4.3, the sharp equatorward edge of the energy dispersions and its uniform motion implies that we observe the ion dispersions after the entire PB crossed the LB or, alternatively, after the cessation of reconnection at the magnetopause. However, using our time-dependent model, we can explore any stage of their evolution.

We discover three distinct phases of the energy dispersions: the "growth" phase, when the dispersion is still forming and is difficult to be identified; the "maturity" phase, when the entire dispersion is present (at least down to the particle energies with significant flux); and the "decline" phase, when the dispersion is disappearing at the low-latitude end due to the finite size of the plasma blob or, equivalently, to the finite duration of reconnection at the magnetopause. These three phases correspond roughly to three time intervals:

$$\begin{cases} & t \ll t_{E,\max} & , \text{ "growth"} \\ t_{E,\max} \lesssim & t < t_{bl} & , \text{ "maturity"} \\ t_{bl} < & t & , \text{ "decline"} \end{cases} \quad (1)$$

where t is the time since the start of precipitation, t_{bl} is the time it takes the entire blob to cross the LB, and $t_{E,\max}$ is the time necessary for the lowest-energy particles with detectable fluxes to reach the spacecraft, in this case around 200 eV. We can see from these inequalities that for the energy dispersion to be clearly and entirely visible we need $t_{bl} \gtrsim t_{E,\max}$. This, in turn, means that the plasma blob has to be big enough in size and/or relatively nearby. These time requirements are consistent with a high-latitude reconnection site. They also require a sufficiently long duration for the reconnection burst.

The full temporal evolution of the two energy dispersions is shown in Plate 4. Snapshots of the latitudinal

profile are shown, representing what a satellite would observe at successive times; the second and third to last frames represent the instances when F8 and F6, respectively, encountered the evolving structures. The three dispersion phases mentioned above are seen clearly in this presentation. Both dispersions are referred to a common time frame, noted above each frame, corresponding to the lifetime of the oldest one (dispersion 2 in Plate 2a).

5. Conclusions

In this paper we proposed a generalized model for reconnection at the dayside magnetopause. It unifies two already well-known processes, the BSXR and MXR models, in a heretofore unique way. MXR operates globally, semicontinuously, and at a low level, while the BSXR is patchy, intermittent, and in the form of enhanced bursts, occurring on top of the MXR background. For convenience we refer to this process as the Bursty Multiple X-Line Reconnection (BMXR) mechanism. Overlapping ion features observed at low altitudes can naturally arise in the context of this new reconnection regime. With correct timing of the BSXR patches, any desired degree of overlap can be easily produced.

Despite its general flexibility, however, we do not claim that the BMXR process is always the dominant magnetopause reconnection mechanism. Other mechanisms, like its isolated component processes, BSXR and MXR, or even steady state reconnection, may at times dominate the flux transfer process. Occasionally, the longitudinal extent of the BMXR process may be limited too, owing to only part of the frontside magnetopause satisfying the required conditions. If the underlying MXR breaks down at a specific longitude, i.e., the secondary x-lines disappear, the plasma blobs forming beyond this point will map down to a significantly dislocated ionospheric position. In fact, several BMXR segments can simultaneously occur at different parts of the magnetopause, separated by simple BSXR or steady state reconnection processes. Our data are unable to address this distinctive possibility, since those disconnected field line footprints will likely fall well outside the satellite paths. Only a cluster of "low-altitude" spacecraft could resolve such ambiguities.

We also developed a particle precipitation model based on a number of simple principles. The independent modeling of the two ion dispersions, a direct consequence of the proposed BMXR process, can easily generate their observed overlap. This demonstrates the feasibility of the BMXR model in this instance and may point to a more general applicability. We argue that the clearest low-altitude particle signature of the BMXR process (and inherently that of the background MXR) is the presence of overlapping ion dispersions. However, we also stress that the interval of easily discerned overlap is a small portion of the entire evolutionary sequence, which complicates the picture. The lack of observed overlap is not necessarily an indicator that BMXR is not operating. It could rather be that the observations were obtained either early or late in the cycle, when overlap is absent or ambiguous.

In summary, the BMXR model is a promising mechanism for dayside magnetopause reconnection. It suggests that all previously proposed reconnection models can be described as different manifestations of a single unifying scheme. Which one dominates at any time is dependent on the magnetopause conditions and the IMF input. Finally, we highlight that the two-point measurements were essential to our analysis and pave the way to future multipoint missions to explore the low-altitude, high-latitude space environment.

Acknowledgments. The authors are grateful to N. U. Crooker for her valuable comments. This work was supported by NASA grant NAG5-4273 and NSF grant ATM-9458424.

Janet G. Luhmann thanks Karlheinz Trattner, Joachim Woch, and another referee for their assistance in evaluating this paper.

References

Biernat, H. K., M. F. Heyn, and V. S. Semenov, Unsteady Petschek reconnection, *J. Geophys. Res., 92,* 3392, 1987.

Burch, J. L., P. H. Reiff, R. A. Heelis, J. D. Winningham, W. B. Hanson, C. Gurgiolo, J. D. Menietti, R. A. Hoffman, and J. N. Barfield, Plasma injection and transport in the mid-altitude polar cusp, *Geophys. Res. Lett., 9,* 921, 1982.

Carlson, C. W., and R. B. Torbert, Solar wind ion injections in the morning auroral oval, *J. Geophys. Res., 85,* 2903, 1980.

Cowley, S. W. H., The causes of convection in the Earth's magnetosphere: A review of developments during the IMS, *Rev. Geophys., 20,* 531, 1982.

Cowley, S. W. H., J. P. Morelli, and M. Lockwood, Dependence of convective flows and particle precipitation in the high-latitude dayside ionosphere on the X and Y components of the interplanetary magnetic field, *J. Geophys. Res., 96,* 5557, 1991a.

Cowley, S. W. H., M. P. Freeman, M. Lockwood, and M. F. Smith, The ionospheric signature of flux transfer events, in *CLUSTER: Dayside polar cusp,* edited by C. I. Barron, *Eur. Space Agency Spec. Publ., ESA SP-330,* 105, 1991b.

Crooker, N. U., An evolution of antiparallel merging, *Geophys. Res. Lett., 13,* 1063, 1986.

Crooker, N. U., J. G. Luhmann, J. R. Spreiter, and S. S. Stahara, Magnetopause merging site asymmetries, *J. Geophys. Res., 90,* 341, 1985.

Dungey, J. W., Interplanetary magnetic field and the auroral zones, *Phys. Rev. Lett., 6,* 47, 1961.

Elphic, R. C., Observations of flux transfer events: A review, in *Physics of the Magnetopause, Geophys. Monogr. Ser.,* vol. 90, edited by P. Song, B. U. Ö. Sonnerup, and M. F. Thomsen, p. 225, AGU, Washington, D. C., 1995.

Escoubet, C. P., M. F. Smith, S. F. Fung, P. C. Anderson, R. A. Hoffman, E. M. Basinska, and J. M. Bosqued, Staircase ion signature in the polar cusp: A case study, *Geophys. Res. Lett., 19,* 1735, 1992.

Fu, Z. F., and L. C. Lee, Simulation of multiple X-line reconnection at the dayside magnetopause, *Geophys. Res. Lett., 12,* 291, 1985.

Fu, Z. F., L. C. Lee, and Y. Shi, A three-dimensional MHD

simulation of the multiple X line reconnection process, in *Physics of Magnetic Flux Ropes, Geophys. Monogr. Ser.*, vol. 58, edited by C. T. Russell, E. R. Priest, and L. C. Lee, p. 515, AGU, Washington, D. C., 1990.

Fuselier, S. A., et al., Bifurcated cusp ion signatures: Evidence for re-reconnection?, *Geophys. Res. Lett., 24,* 1471, 1997.

Gosling, J. T., J. R. Asbridge, S. J. Bame, W. C. Feldman, G. Paschmann, N. Sckopke, and C. T. Russell, Evidence for quasi-stationary reconnection at the dayside magnetopause, *J. Geophys. Res., 87,* 2147, 1982.

Haerendel, G., G. Paschmann, N. Sckopke, H. Rosenbauer, and P. C. Hedgecock, The frontside boundary layer of the magnetosphere and the problem of reconnection, *J. Geophys. Res., 83,* 3195, 1978.

Hardy, D. A., L. K. Schmitt, M. S. Gussenhoven, F. J. Marshall, H. C. Yeh, T. L. Schumaker, A. Huber, and J. Pantazis, Precipitating electron and ion detectors (SSJ/4) for the block 5D/flight 6-10 DMSP satellites: Calibration and data presentation, *Rep. AFGL-TR-84-0314,* Air Force Geophys. Lab., Hanscom Air Force Base, Mass., 1984.

Jorgensen, A. M., and H. E. Spence, On separating space and time variations of auroral precipitation: Dual DMSP-F6 and -F8 observations, *Adv. Space Res., 20,* (3), 453, 1997.

Jorgensen, A. M., H. E. Spence, T. J. Hughes, and D. McDiarmid, A study of Omega bands and PS-6 pulsations on the ground, at low-altitude, and at geostationary orbit, *J. Geophys. Res., 104,* 14,705, 1999.

Kan, J. R., A theory of patchy and intermittent reconnections for magnetospheric flux transfer events, *J. Geophys. Res., 93,* 5613, 1988.

La Belle-Hamer, A. L., Z. F. Fu, and L. C. Lee, A mechanism for patchy reconnection at the dayside magnetopause, *Geophys. Res. Lett., 15,* 152, 1988.

Lee, L. C., and Z. F. Fu, A theory of magnetic flux transfer at the Earth's magnetopause, *Geophys. Res. Lett., 12,* 105, 1985.

Lee, L. C., and Z. F. Fu, Multiple X line reconnection, 1, A criterion for the transition from a single X line to a multiple X line reconnection, *J. Geophys. Res., 91,* 6807, 1986.

Lee, L. C., Z. W. Ma, Z. F. Fu, and A. Otto, Topology of magnetic flux ropes and formation of fossil flux transfer events and boundary layer plasmas, *J. Geophys. Res., 98,* 3943, 1993.

Lockwood, M., Overlapping cusp ion injections: An explanation invoking magnetopause reconnection, *Geophys. Res. Lett., 22,* 1141, 1995a.

Lockwood, M., Location and characteristics of the reconnection X line deduced from low-altitude satellite and ground-based observations, 1, Theory, *J. Geophys. Res., 100,* 21,791, 1995b.

Lockwood, M., and C. J. Davis, On the longitudinal extent of magnetopause reconnection pulses, *Ann. Geophys., 14,* 865, 1996.

Lockwood, M., and M. F. Smith, The variation of reconnection rate at the dayside magnetopause and cusp ion precipitation, *J. Geophys. Res., 97,* 14,841, 1992.

Lockwood, M., and M. F. Smith, Low and middle altitude cusp particle signatures for general magnetopause reconnection rate variations, 1, Theory, *J. Geophys. Res., 99,* 8531, 1994.

Lockwood, M., C. J. Davis, M. F. Smith, T. G. Onsager, and W. F. Denig, Location and characteristics of the reconnection X line deduced from low-altitude satellite and ground-based observations, 2, Defense Meteorological Satellite Program and European Incoherent Scatter data, *J. Geophys. Res., 100,* 21,803, 1995.

Lockwood, M., C. J. Davis, T. G. Onsager, and J. D. Scudder, Modelling signatures of pulsed magnetopause reconnection in cusp ion dispersion signatures seen at middle altitudes, *Geophys. Res. Lett., 25,* 591, 1998.

Luhmann, J. G., R. J. Walker, C. T. Russell, N. U. Crooker, J. R. Spreiter, and S. S. Stahara, Patterns of potential magnetic field merging sites on the dayside magnetopause, *J. Geophys. Res., 89,* 1739, 1984.

Newell, P. T., and C.-I. Meng, The cusp and the cleft/boundary layer: Low altitude identification and statistical local time variation, *J. Geophys. Res., 93,* 14,549, 1988.

Newell, P. T., and C.-I. Meng, Ion acceleration at the equatorward edge of the cusp: Low altitude observations of patchy merging, *Geophys. Res. Lett., 18,* 1829, 1991.

Newell, P. T., and C.-I. Meng, Cusp low-energy ion cutoffs: A survey and implications for merging, *J. Geophys. Res., 100,* 21,943, 1995.

Newell, P. T., and S. Wing, Entry of solar wind plasma into the magnetosphere: Observations encounter simulation, in *Geospace Mass and Energy Flow: Results from the International Solar-Terrestrial Physics Program, Geophys. Monogr. Ser.,* vol. 104, edited by J. L. Horwitz, D. L. Gallagher, and W. K. Peterson, p. 73, AGU, Washington, D. C., 1998.

Newell, P. T., W. J. Burke, C.-I. Meng, E. R. Sanchez, and M. E. Greenspan, Identification and observations of the plasma mantle at low altitude, *J. Geophys. Res., 96,* 35, 1991.

Nishida, A., Can random reconnection at the magnetopause produce the low latitude boundary layer?, *Geophys. Res. Lett., 16,* 227, 1989.

Norberg, O., M. Yamauchi, L. Eliasson, and R. Lundin, Freja observations of multiple injection events in the cusp, *Geophys. Res. Lett., 21,* 1919, 1994.

Ogino, T., R. J. Walker, and M. Ashour-Abdalla, A magnetohydrodynamic simulation of the formation of magnetic flux tubes at the Earth's dayside magnetopause, *Geophys. Res. Lett., 16,* 155, 1989.

Onsager, T. G., C. A. Kletzing, J. B. Austin, and H. MacKiernan, Model of magnetosheath plasma in the magnetosphere: Cusp and mantle particles at low altitudes, *Geophys. Res. Lett., 20,* 479, 1993.

Onsager, T. G., S.-W. Chang, J. D. Perez, J. B. Austin, and L. X. Janoo, Low-altitude observations and modeling of quasi-steady magnetopause reconnection, *J. Geophys. Res., 100,* 11,831, 1995.

Paschmann, G., G. Haerendel, I. Papamastorakis, N. Sckopke, S. J. Bame, J. T. Gosling, and C. T. Russell, Plasma and magnetic field characteristics of magnetic flux transfer events, *J. Geophys. Res., 87,* 2159, 1982.

Phillips, J. L., S. J. Bame, R. C. Elphic, J. T. Gosling, M. F. Thomsen, and T. G. Onsager, Well-resolved observations by ISEE 2 of ion dispersion in the magnetospheric cusp, *J. Geophys. Res., 98,* 13,429, 1993.

Pinnock, M., A. S. Rodger, J. R. Dudeney, F. Rich, and K. B. Baker, High spatial and temporal resolution observations of the ionospheric cusp, *Ann. Geophys., 13,* 919, 1995.

Reiff, P. H., T. W. Hill, and J. L. Burch, Solar wind plasma injection at the dayside magnetospheric cusp, *J. Geophys. Res., 82,* 479, 1977.

Rijnbeek, R. P., S. W. H. Cowley, D. J. Southwood, and C. T. Russell, A survey of dayside flux transfer events observed by ISEE 1 and 2 magnetometers, *J. Geophys. Res., 89,* 786, 1984.

Rosenbauer, H., H. Gruenwaldt, M. D. Montgomery, G. Paschmann, and N. Sckopke, HEOS-2 plasma observations in the distant polar magnetosphere: The plasma mantle, *J. Geophys. Res., 80,* 2723, 1975.

Russell, C. T., and R. C. Elphic, Initial ISEE magnetometer results: Magnetopause observations, *Space Sci. Rev., 22,* 681, 1978.

Russell, C. T., and R. C. Elphic, ISEE observations of flux transfer events at the dayside magnetopause, *Geophys. Res. Lett., 6,* 33, 1979.

Sato, T., T. Shimada, M. Tanaka, T. Hayashi, and K. Watanabe, Formation of field-twisting flux tubes on the magnetopause and solar wind particle entry into the magnetosphere, *Geophys. Res. Lett., 13,* 801, 1986.

Saunders, M. A., Recent ISEE observations of the magnetopause and low latitude boundary layer: A review, *J. Geophys., 52,* 190, 1983.

Scholer, M., Magnetic flux transfer at the magnetopause based on single X-line bursty reconnection, *Geophys. Res. Lett., 15,* 291, 1988a.

Scholer, M., Strong core magnetic fields in magnetopause flux transfer events, *Geophys. Res. Lett., 15,* 748, 1988b.

Scholer, M., Asymmetric time-dependent and stationary magnetic reconnection at the dayside magnetopause, *J. Geophys. Res., 94,* 15,099, 1989.

Scholer, M., Models of flux transfer events, in *Physics of the Magnetopause, Geophys. Monogr. Ser.,* vol. 90, edited by P. Song, B. U. Ö. Sonnerup, and M. F. Thomsen, p. 235, AGU, Washington, D. C., 1995.

Shi, Y., C. C. Wu, and L. C. Lee, A study of multiple X line reconnection at the dayside magnetopause, *Geophys. Res. Lett., 15,* 295, 1988.

Shi, Y., C. C. Wu, and L. C. Lee, Magnetic field reconnection patterns at the dayside magnetopause: An MHD simulation study, *J. Geophys. Res., 96,* 17,627, 1991.

Smith, M. F., and M. Lockwood, The pulsating cusp, *Geophys. Res. Lett., 17,* 1069, 1990.

Smith, M. F., and M. Lockwood, Earth's magnetospheric cusps, *Rev. Geophys., 34,* 233, 1996.

Smith, M. F., M. Lockwood, and S. W. H. Cowley, The statistical cusp: A flux transfer event model, *Planet. Space Sci., 40,* 1251, 1992.

Sonnerup, B. U. Ö., On the stress balance in flux transfer events, *J. Geophys. Res., 92,* 8613, 1987.

Southwood, D. J., C. J. Farrugia, and M. A. Saunders, What are flux transfer events?, *Planet. Space Sci., 36,* 503, 1988.

Spreiter, J. R., and S. S. Stahara, Magnetohydrodynamic and gasdynamic theories for planetary bow waves, in *Collisionless Shocks in the Heliosphere: Reviews of Current Research, Geophys. Monogr. Ser.,* vol. 35, edited by B. T. Tsurutani and R. G. Stone, p. 85, AGU, Washington, D. C., 1985.

Trattner, K. J., A. J. Coates, A. N. Fazakerley, A. D. Johnstone, H. Balsiger, J. L. Burch, S. A. Fuselier, W. K. Peterson, H. Rosenbauer, and E. G. Shelley, Overlapping ion populations in the cusp: Polar/TIMAS results, *Geophys. Res. Lett., 25,* 1621, 1998.

Watermann, J., O. De la Beaujardiere, and H. E. Spence, Space-time structure of the morning aurora inferred from coincident DMSP-F6, -F8, and Sondrestrom incoherent scatter radar observations, *J. Atmos. Terr. Phys., 55,* 1729, 1993.

Woch, J., and R. Lundin, Temporal magnetosheath plasma injection observed with Viking: A case study, *Ann. Geophys., 9,* 133, 1991.

Woch, J., and R. Lundin, Signatures of transient boundary layer processes observed with Viking, *J. Geophys. Res., 97,* 1431, 1992.

Xue, S., P. H. Reiff, and T. G. Onsager, Mid-altitude modeling of cusp ion injection under steady and varying conditions, *Geophys. Res. Lett., 24,* 2275, 1997.

Yamauchi, M., and R. Lundin, Classification of large-scale and meso-scale ion dispersion patterns observed by Viking over the cusp-mantle region, in *Physical Signatures of Magnetospheric Boundary Layer Processes,* edited by J. A. Holtet and A. Egeland, p. 99, Kluwer Acad., Norwell, Mass., 1994.

A. Boudouridis, Department of Atmospheric Sciences, University of California, Los Angeles, 405 Hilgard Avenue, Los Angeles, CA 90095, USA. (thanasis@atmos.ucla.edu)

T. G. Onsager, Space Environment Center, NOAA, 325 Broadway, Boulder, CO 80303, USA. (tonsager@sec.noaa.gov)

H. E. Spence, Center for Space Physics, Boston University, 725 Commonwealth Avenue, Boston, MA 02215, USA. (spence@bu.edu)

(Received September 13, 2000; revised May 24, 2001; accepted May 24, 2001.)